

# Observation of structures in the invariant masses of two nucleons in the disintegration of the deuteron by protons

V. P. Andreev, A. V. Kravtsov, M. M. Makarov, V. I. Medvedev,  
G. Z. Obrant, V. I. Poromov, V. V. Sarantsev, G. L. Sokolov,  
A. B. Sokornov, and S. G. Sherman

*B. P. Konstantinov Institute of Nuclear Physics, Academy of Sciences of the USSR*

(Submitted 14 April 1987)

*Pis'ma Zh. Eksp. Teor. Fiz.* **45**, No. 11, 508–510 (10 June 1987)

The effective-mass spectra of two nucleons in the reaction  $pd \rightarrow ppn$ , in which one of the nucleons is emitted into the rear hemisphere, have been studied. A selection of events with large momenta and/or large angles between the nucleon emission directions in the spectra of  $M_{pn}$  and  $M_{pp}$  reveals several narrow structural features ( $M = 1.95, 2.03, 2.08, \text{ and } 2.14 \text{ GeV}/c^2$ ).

Reports of the observation of narrow structural features in the effective-mass spectra of two-nucleon systems produced in  $NN$  collisions and in particle-nucleus interactions have recently attracted particular interest. These features are regarded as candidates for dibaryon resonances.<sup>1</sup>

In this letter we report a study of the effective-mass spectra of two nucleons in the disintegration of the deuteron by protons at four energies of the impinging proton ( $p_0 = 1.438, 1.503, 1.561, \text{ and } 1.669 \text{ GeV}/c$ ).

The experiments were carried out at the synchrocyclotron of the Leningrad Institute of Nuclear Physics with a 35-cm bubble chamber filled with deuterium.<sup>2</sup> When the films were examined, two-pronged events, in which one of the protons was emitted into the rear hemisphere with respect to the beam, were selected. An important limitation is that events with proton momenta below  $80 \text{ MeV}/c$  are not seen in the bubble chamber. The number of deuteron disintegration events analyzed was  $8 \times 10^3$ ; the numbers of events for the various energies were approximately the same.

All events were divided into two classes<sup>3</sup> on the basis of which particle—the proton or the neutron—in the final state had the higher energy: “charge-conservation reactions” and “charge-exchange reactions,” respectively. The effective-mass distribution was constructed for the remaining two nucleons; i.e., in the first set of events we studied the  $M_{pn}$  spectrum, and in the second we studied the  $M_{pp}$  spectrum.

We know quite well that the overwhelming majority of deuteron disintegration events are events of quasielastic scattering. Phenomena which are caused by a different physics, in particular, by possible dibaryon resonance, should be sought where the deuteron interacts as a whole. One way to suppress the contribution of quasielastic scattering would be to select events in which the momenta of the nucleons are fairly large. Figure 1, a–d, shows distributions in the effective mass  $M_{pn}$ , summed over the four energies, for sets of events in which the momentum of the slowest nucleon is above 80, 150, 200, and 250  $\text{MeV}/c$ , respectively. From the changes in these spectra

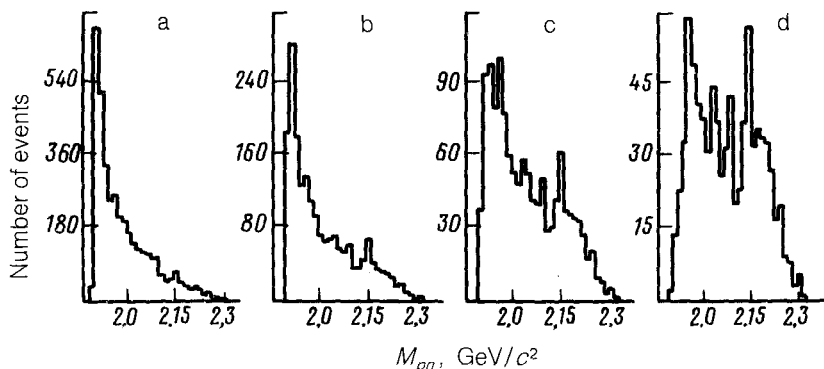


FIG. 1. Distribution in the effective mass  $M_{pn}$  of "charge-conservation-reaction" events. a—The momenta of the nucleons satisfy  $p > 80$  MeV/c; b— $p > 150$  MeV/c; c— $p > 200$  MeV/c; d— $p > 250$  MeV/c.

we see that as the limitation on the magnitude of the momentum is intensified, the main peak (at the extreme left), which is due to quasielastic scattering, decreases in size. It disappears completely for events with a nucleon momentum  $p > 250$  MeV/c. At the same time, some narrow structural features appear in the spectrum. The positions of these features coincide (as a further analysis shows) with the candidates for dibaryon resonances which have been observed in other experiments.<sup>1</sup>

Another way to distinguish possible resonances against the background of quasielastic scattering might be based on the following arguments. Since most of the energy in the final state is carried off by the nucleon which is eliminated from consideration during the construction of the spectra, the resonance states which are produced should have a small kinetic energy, so that their decay products would be emitted at large angles in the laboratory frame of reference. Figure 2, a-c, shows distributions in the effective mass  $M_{pp}$ , summed over all energies, for all events and also for the sets of

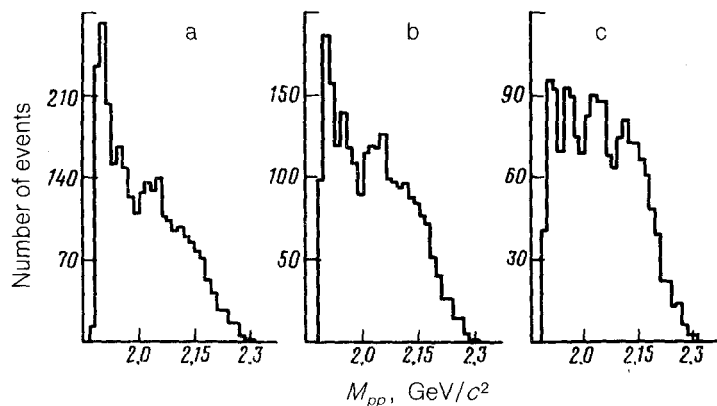


FIG. 2. Distributions in the effective mass  $M_{pp}$  of "charge-exchange-reaction" events. a—The entire range of proton emission angles; b— $\psi_{pp} > 90^\circ$ ; c— $\psi_{pp} > 120^\circ$ .

events in which the proton scattering angle was  $\Psi_{pp} > 90^\circ$  or  $\Psi_{pp} > 120^\circ$ . We see that the changes in the spectra are similar to those seen in Fig. 1: The same structural features appear in the spectra.

Observation of the effects through the use of two independent selection criteria—an energy criterion and an angular criterion—provides evidence that these effects are of a physical (rather than kinematic) nature.

Using the limitations described above on the momenta and angles (both separately and jointly), we find that four narrow structural features appear in the  $M_{pn}$  spectra, at a level of no less than three standard deviations, while only three features appear in the  $M_{pp}$  spectrum. These structural features are also observed in the spectra for each energy, but the statistical base is unreliable in those cases. Our resolution in terms of the effective mass  $M_{pp}$  varies smoothly from a few MeV near the threshold to 10–15 MeV at  $2.15 \text{ GeV}/c^2$  and then increases sharply up to 30 MeV. In the case of the  $M_{pn}$ , the resolutions at 5 and 10 MeV, respectively, are poorer. It may be that the poor resolution above  $2.15 \text{ GeV}/c^2$  is preventing us from seeing anything in this region, although reports of some studies indicate that there are also structural features here. In a first approximation, we eliminated the large-mass region ( $M_{NN} > 2.18 \text{ GeV}/c^2$ ) in determining the positions of the structural features.

The spectra of the effective mass  $M_{pn}$  ( $M_{pp}$ ) were fitted by a function consisting of the sum of four (or three) Breit-Wigner functions and a background in the form of a second-degree polynomial. Examples of a fit of this type are shown in Fig. 3, where the solid line is the overall result of an incoherent summation, while the dashed line is the background. As a result of the fit of the  $M_{pn}$  spectra, we found the following characteristics for the resonance structures:

$$M = 1953 \pm 2, \quad \Gamma = 32 \pm 3 \text{ MeV}; \quad M = 2024 \pm 3, \quad \Gamma = 33 \pm 4 \text{ MeV};$$

$$M = 2079 \pm 4, \quad \Gamma = 10 \pm 6 \text{ MeV}; \quad M = 2144 \pm 7, \quad \Gamma = 22 \pm 2 \text{ MeV}.$$

From the  $M_{pp}$  spectra we find  $M = 1956 \pm 3$ ,  $\Gamma = 17 \pm 5 \text{ MeV}$ ,  $M = 2035 \pm 8$ ,  $\Gamma = 39 \pm 11 \text{ MeV}$ ,  $M = 2104 \pm 9$ , and  $\Gamma = 45 \pm 5 \text{ MeV}$ . The positions of the resonance features remain quite stable when they are determined from different kinematic regions. In the  $M_{pn}$  spectrum there is a resonance peak at  $2.08 \text{ GeV}/c^2$ , while we do not see it in the  $M_{pp}$  spectrum. A possible reason is that in the  $M_{pp}$  system two structural features, at  $2.08$  and  $2.14 \text{ GeV}/c^2$ , coalesce (e.g., each feature broadens because of a Coulomb repulsion), and at our resolution they cannot be distinguished. There is another possible explanation, however: Mulders *et al.*<sup>4</sup> predict a narrow resonance in this region, in a channel with an isospin  $I = 0$ . In this case, it would not contribute to the  $M_{pp}$  spectrum.

As can be seen from Fig. 3a, the high-energy part of the  $M_{pn}$  spectrum is not described satisfactorily. When we added one more resonance in this region, we found a satisfactory ( $\chi^2/DF = 1.2$ ) description of the entire spectrum (the dashed line in Fig. 3a; the dot-dashed line is the new background). The values of the parameters of this additional resonance are  $M = 2193 \pm 4$  and  $\Gamma = 58 \pm 8 \text{ MeV}$ .

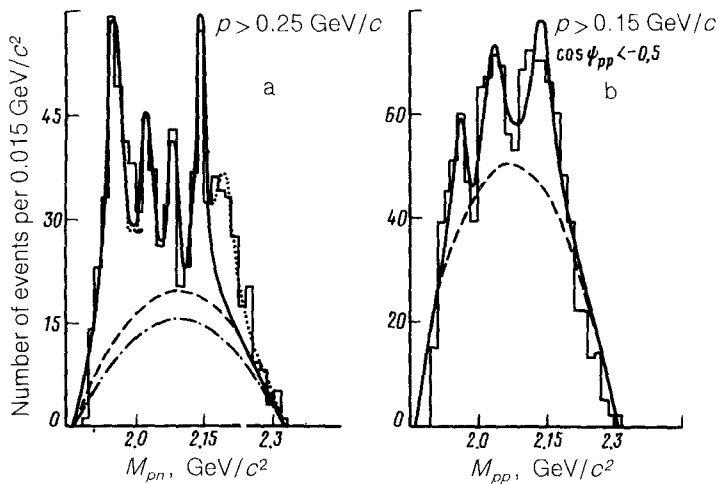


FIG. 3. a— $M_{pn}$  distribution for events with nucleon momenta above 250 MeV/c; b— $M_{pp}$  distribution for events with proton momenta above 150 MeV/c and with  $\Psi_{pp} > 120^\circ$ .

The observed structural features fit well into the rotational bands of the multi-quark bag model.<sup>4</sup>

<sup>1</sup>A. Svarc, Nucl. Phys. **A434**, 329 (1985); B. Tatischeff, Nucl. Phys. **A446**, 355 (1985).

<sup>2</sup>V. P. Andreev *et al.*, Yad. Fiz. **42**, 1420 (1985) [Sov. J. Nucl. Phys. **42**, 899 (1985)].

<sup>3</sup>B. S. Aladashvili, Nucl. Phys. **A274**, 486 (1976).

<sup>4</sup>P. J. Mulders *et al.*, Phys. Rev. D **21**, 2653 (1980).

Translated by Dave Parsons